

Evaluation of silicon microstrip detectors as X-ray sensors in digital mammography

Tadej Mali¹, Vladimir Cindro¹, Marko Mikuž^{1,2},
Urban Zdešar³, and Breda Jančar⁴

¹Jožef Stefan Institute, ²University of Ljubljana, Faculty of Mathematics and Physics, Department of Physics, ³Institute of Occupational Safety, Republic of Slovenia, ⁴Institute of Oncology, Slovenia

Background. Position sensitive silicon microstrip detectors are used as sensors for X-rays in a digital imaging system. Silicon detectors were used in an edge-on geometry, yielding high X-ray detection efficiency.

Material and methods. A small detector system was assembled and tested. Images of a standard, 5 cm thick phantom were made and evaluated. It is demonstrated, that the use of silicon detectors in mammography could significantly contribute to a reduction of dose. All images were made with skin entrance doses lower than 1 mGy.

Results and conclusion. Microcalcifications with a diameter of 350 μm could still be detected with skin entrance doses of about 0.25 mGy. It was demonstrated that a 5 lp/mm pattern can be detected. Image processing should further improve the image quality.

Key words: mammography; radiographic image enhancement; silicon

Introduction

Silicon microstrip detectors are position sensitive detectors, intrinsically developed for high precision tracking in particle physics. Recently they were proposed to be used as X-ray detectors in full field digital mammography.^{1,2,3}

Their advantage over screen-film is in

higher X-ray detection efficiency, leading to a reduction of the dose required per investigation. In addition, the proposed edge-on geometry suppresses the detection of radiation scattered in the tissue, thus increases the quality of radiographic images. The microstrip detectors operate in a single photon counting mode. If low noise electronics is used for photon counting, the noise in the image is due to statistical fluctuations of the number of detected photons only. However, the expected spatial resolution is somewhat lower than in the case of screen-film.

We have constructed and built a small test system. Several images of phantoms were

Received 14 April 1999

Accepted 21 July 1999

Correspondence to: Tadej Mali, Jožef Stefan Institute, Jamova 39, SI-1000 Ljubljana, Slovenia. Phone: +386 61 177 3832; Fax: +386 61 125 70 74; E-mail: Tadej.Mali@ijs.si

recorded and quality of images was evaluated to check the system performance.

Material and methods

Silicon microstrip detectors

The silicon microstrip detector is an array of closely spaced semiconducting p+n junctions - strips. Under reverse bias the p+n junction is depleted of free carriers and every photon interacting in the depleted region generates a current pulse which can be detected. In our system every strip of the detector is bonded to a readout circuit, where a fast preamplifier is followed by a discriminator and 16 bit counter. When the amplified signal exceeds a user defined threshold of the discriminator, the content of the counter is incremented by one.

The absorption length of X-ray photons in silicon in the energy range of interest (around 20 keV) is approximately 1 mm. In 3 mm of silicon as much as $1 - e^{-3} = 95\%$ of radiation is absorbed. Therefore an active detector depth of a few millimeters is sufficient for high efficiency. Silicon detectors are typically fabricated on 200 to 300 μm thick wafers while the length of strips can be up to several centime-

ters. If the incoming photons hit the detector from the side (Figure 1), the whole length of the strip is available for photon absorption. Practically all incoming radiation is absorbed in the detector and the detection efficiency is very high.^{1,2,3} This is called an "edge-on geometry".

However, the active volume of the device cannot extend completely to the edge of the silicon substrate. Surface damage due to cutting would increase the dead current in the device, resulting in an increase of noise, leading to false photon counts.¹ Therefore a guard ring structure around the strips and a safety distance between the structures and cutting edge are required. They represent the inactive volume of the detector, because the photons, absorbed in the region between the cutting edge and the strips, cannot be detected (Figure 1). Detection efficiency (η) is therefore limited by the thickness of dead volume (t) as $\eta = e^{-\mu t}$, where μ is the absorption coefficient for X-rays in silicon.

In the detector used for this experiment the dead region was 600 μm thick, giving 55% efficiency at 20 keV. Measurements have shown, however, that the dead region could be reduced to values between 100 and 200 μm , giving 90-80% efficiency at 20 keV.^{2,4}

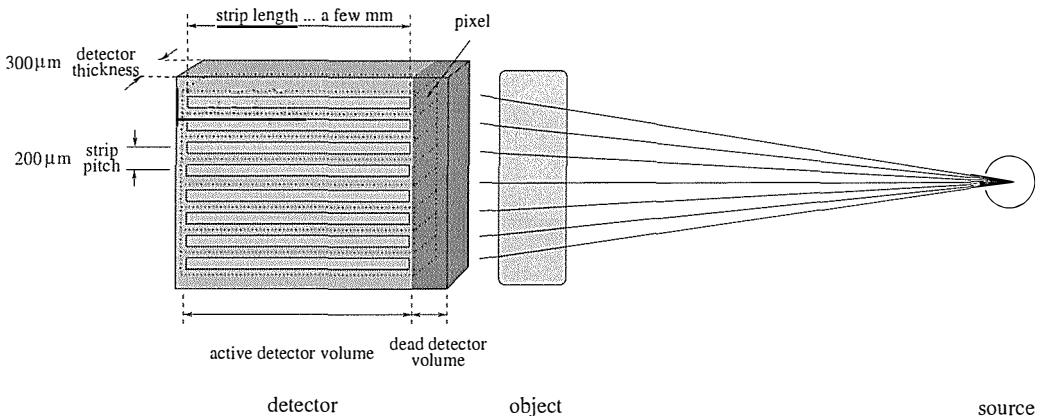


Figure 1. Silicon microstrip detector used in the 'edge-on' geometry. X-ray photons emerge from the source on the right hand side of the figure.

In the "edge-on geometry" a single microstrip detector acts as a linear pixel detector (one row of pixels) with the pixel dimensions given by the strip pitch (typically 25 to 200 μm) and the detector thickness (200 to 300 μm).

The pixel dimensions of the detector used in our study were $100 \times 300 \mu\text{m}^2$ and the system consisted of 31 strips of a single microstrip detector, resulting in a row of pixels covering an area of $3.1 \times 0.3 \text{ mm}^2$. To obtain 2D images the object was moved in the direction perpendicular to the detector plane and an image of a narrow slice was taken at every step. To minimize the dose received by the patient during imaging, the X-ray beam must be collimated by a slit in such a way, that the radiation field fits the area covered by the detector. This imaging technique is called slit-scanning.

Readout electronics

The readout electronics of the device is a custom designed readout circuit CASTOR, developed by LEPSI, Strasbourg. CASTOR is a VLSI mixed analog-digital circuit consisting of 32 parallel independent channels, capable of single photon counting. The circuit enables photon counting without false photon hits for photon energies above 12 keV. The circuit and its operation are described in details elsewhere.^{5,6,7,8}

Imaging system

As already mentioned, the silicon detector covered an area of $3.1 \times 0.3 \text{ mm}^2$, which is much smaller than objects under investigation. Therefore images of the objects were obtained by scanning the object positioned on a table, moved by a step motor. In this way images of narrow (3.1 mm in y direction), long (a few cm in x direction) regions were obtained (Figure 2).^{7,8}

The spatial resolution depends on the pixel

size as well as on the sampling rate. The sampling rate in the direction along the detector (y axis in Figure 2) was determined by the strip pitch. The sampling rate in the direction of scanning (x axis in Figure 2) was equal to the scanning step and could be varied. Different scanning steps ranging from 50 to 300 μm were used. The position of the detector and X-ray source were kept fixed. The scanning and readout of the device were controlled by a personal computer.

The X-ray source was an X-ray tube with a tungsten electrode operated at 32 kV_p and the cathode current was 5 mA. The first half value layer of aluminum was measured to be 0.8 mm. Note that neither the operating voltage nor the anode material were optimal for mammography. Optimization of these parameters would result in even better contrast and lower dose.⁹ The distance between the source and the phantom was 60 cm.

The entrance skin dose was measured on a 4.5 cm thick PMMA phantom using a thin window parallel plate ionization chamber PS-033 together with a Capintec WK 192 electrometer. The dose rate on the phantom at the given position was $3.3 \pm 0.3 \text{ mGy/min}$.

The phantom was a 5 cm thick "CIRS Tissue Equivalent Phantom Model 11". It was made of breast tissue equivalent plastic (30% gland, 70% adipose). Microcalcifications were modeled by irregularly shaped pieces of CaCO_3 embedded in the phantom.

Results

Images of small, high contrast objects

Contrast was studied by imaging a group of small, high contrast objects - microcalcifications with a diameter of 350 μm . Their image was obtained at different levels of exposure in order to study the detection limit. The contrast of the objects, C was defined as:

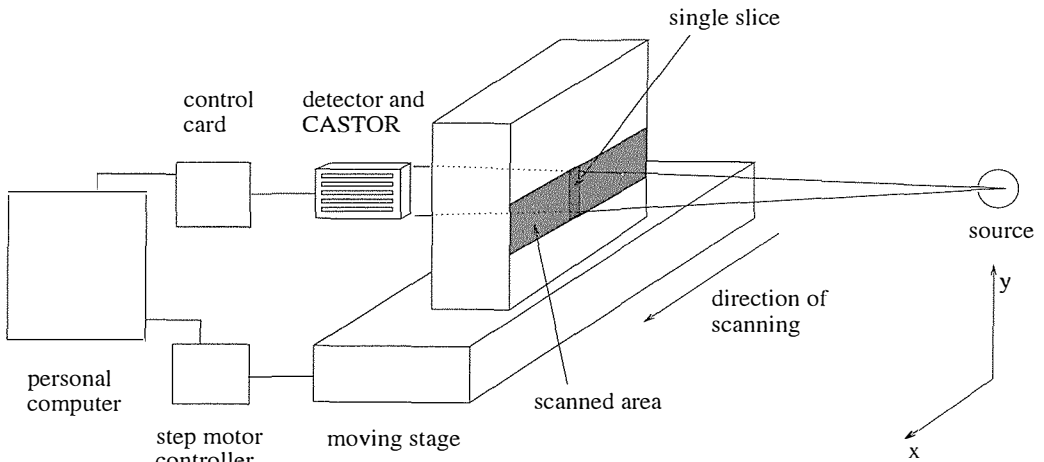


Figure 2. X-ray imaging setup. An object was positioned on the moving stage, while the position of the X-ray source and detector was fixed. An image of a narrow (3.1 mm in y direction) region of the object is obtained by scanning in x direction.

$$C = \frac{N_1 - N_2}{N_1}$$

where N_1 is the number of detected photons per pixel in the region without microcalcifications (background region) and N_2 is the minimum number of detected photons per pixel in the region, of the microcalcification (signal region).

A detail of the phantom, showing a cluster of microcalcifications is shown in Figure 3. The size of y axis was given by the number of channels and the strip pitch (31×0.1 mm) and the x axis was determined by the scanning direction and step size (50×0.2 mm). The image in Figure 3 was obtained at 1.0 ± 0.1 mGy skin entrance dose. Figure 3a shows an image of three microcalcifications, which can be seen as white spots. Figure 3b shows the number of counts per pixel at $y=2.1$ mm. Because of the amplifier gain variations between channels of the circuit, the number of detected photons varies too (up to 15%). Therefore the average number of hits in the background region of every single channel was calculated and the number of hits was normalized to this average.

The average number of detected photons

per pixel was about 26000 in the background and 24500 in the signal area. Using these numbers the contrast of the microcalcification at position $x=3.5$, $y=2.1$ was estimated to be

$$C = \frac{26000 - 24500}{26000} \approx 6\%.$$

One expects that the number of detected photons per pixel is given by the Poisson distribution, yielding the standard deviation of $\sqrt{26000} \approx 160$. Thus relative fluctuations of the background are about 0.6% in agreement with Figure 3.

The same detail was also observed with different levels of exposure, ranging from 1.0 to 0.16 mGy of skin entrance dose (Figure 4). The microcalcifications are clearly detectable at a dose of about 0.25 mGy and even at lower dose (0.16 mGy) they can still be recognized.

One can see in Figure 3 that the average number of detected photons at $x>5$ is somewhat lower, which is due to the source intensity variations in time. Since the image is obtained by scanning, the instability of current in the X-ray source is manifested as the background variation along the x axis. The low exposure rate (3.3 ± 0.3 mGy/min) result-

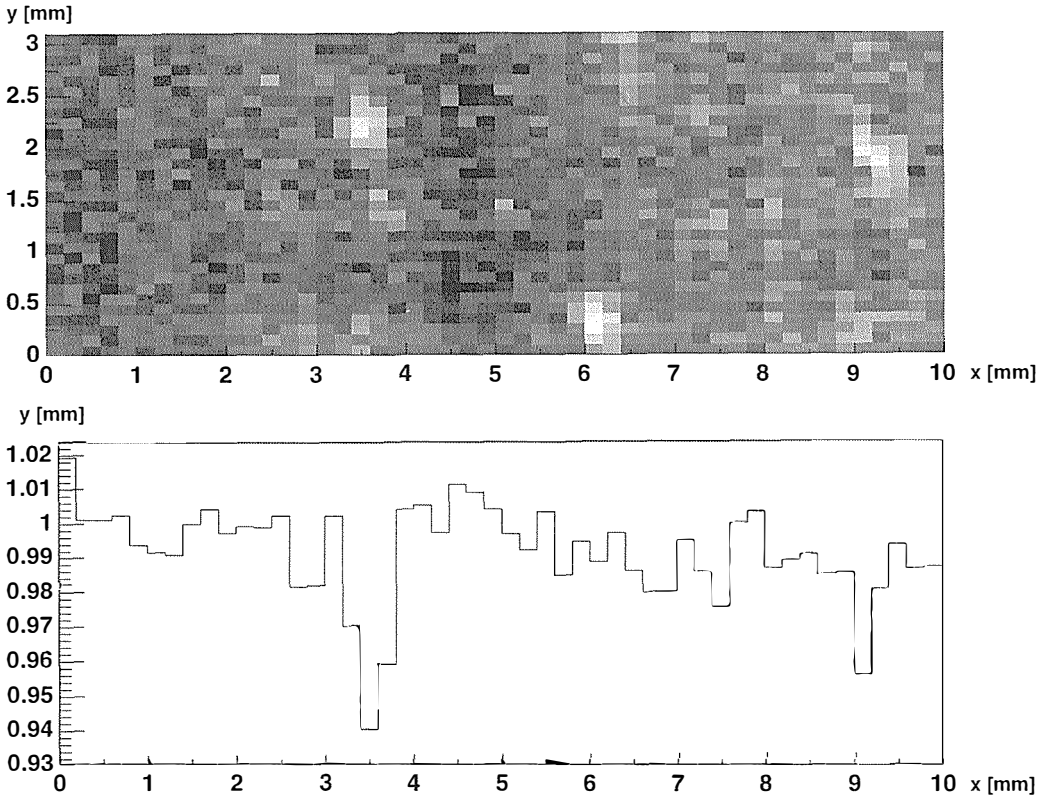


Figure 3. Microcalcifications with a diameter of $350 \mu\text{m}$. The contrast of the object at $x=3.5$ is 6%. The image was obtained by scanning in x direction with a scanning step of $200 \mu\text{m}$; the strip pitch of the detector was $100 \mu\text{m}$. The size of pixels is $300 \times 100 \mu\text{m}^2$ ($x \times y$ size). The image was obtained at a skin entrance dose of 1 mGy .

In Figure 3a three microcalcifications can be seen at positions: ($x=6, y=0.25$), ($x=3.5, y=2.15$) and ($x=9.2, y=1.8$). A cut through Figure 3a at $y=2.15$ is shown in Figure 3b.

ed in an exposure time per step of 12 s and a total of 10 min was required for the whole image.

Spatial resolution

Spatial resolution of the imaging system was studied by imaging a series of high contrast linepairs (lp) with different spatial frequencies. The spatial resolution of the system is characterized by the maximum spatial frequency (ν) of the linepair detail, that can still be detected. Among other it is limited by the size of the pixel which is relatively large - $100 \times 300 \mu\text{m}^2$. However, appropriate scanning steps could improve the spatial resolution in

one direction. The spatial resolution is limited by the Nyquist criteria¹⁰:

$$\nu_{\text{max}} = \frac{1}{2d},$$

where ν_{max} is the maximal spatial frequency, which can be detected when a spatially variable signal is sampled at discrete, equidistant points, separated by distance d . In the direction along the detector, the maximum space frequency was limited by the strip pitch ($100 \mu\text{m}$), yielding the limit of 5 lp/mm in our case. The spatial resolution in the direction of scanning could be varied by changing the size of scanning step. The scanning step used for detection of microcalcifications in Figures 3

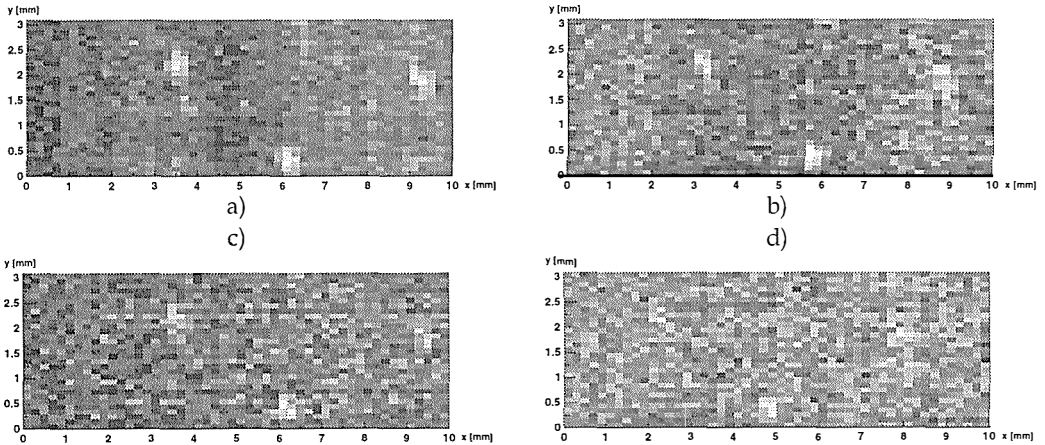


Figure 4. Cluster of microcalcifications with diameter of 350 μm imaged at different level of exposure. Figure 4a: 1 mGy, Figure 4b: 0.5 mGy, Figure 4c: 0.25 mGy and Figure 4d 0.16 mGy. Microcalcifications are clearly visible at skin entrance dose of 0.25 mGy and can still be detected at a dose of 0.16 mGy.

and 4 was 200 μm , giving the maximum frequency of 2.5 lp/mm in x direction. These numbers are significantly worse than in the case of screen-film (above 10 lp/mm). To enable the detection of 10 lp/mm spatial frequency, the strip pitch as well as the scanning step should be scaled down to 50 μm .

In order to demonstrate the spatial resolution improvement by a finer scanning step, we made a measurement with a scanning step of 50 μm (Figure 5), theoretically enabling detection of a 10 lp/mm pattern. Figure 5 shows the phantom detail, where a 5 lp/mm pattern is clearly visible.

However, the size of pixel (300 μm in direction of scanning) distorts the image (Figure 5). Instead of five lines, standing out of the background, the figure shows a plateau and four lines standing out from the background. The plateau is obtained when a pixel covers a white-black-white pattern and the peaks are obtained when a pixel covers a black-white-black pattern of the phantom. Therefore the modulation transfer function (MTF) of the system should be evaluated and further image processing is required to achieve higher spatial resolution without distortion.

Discussion

The presented results show that the silicon microstrip detectors, used in the edge-on geometry, can be successfully exploited as an X-ray detector in full field digital mammography.

Images of rather large (350 μm) microcalcifications were obtained. As expected, the noise in the image is mainly due to statistical fluctuations. The estimated contrast of the objects was low: 5-8%. This is mostly attributed to Compton scattering in the object. The contrast could be improved by using a slit, which would reject the Compton scattered photons. In addition the hardness of the radiation used was rather large. The first half value layer of Al was 0.8 mm, while in conventional mammograms it is 0.3-0.4 mm only¹².

Even with this non optimized geometry (no slits for Compton scattering rejection), large edge cut (600 μm) and the non ideal radiation source (spectrum too hard), phantom objects were recognized with skin entrance doses lower than 0.25 mGy, which is significantly less than the dose required for the screen-film combination (>3 mGy). It is

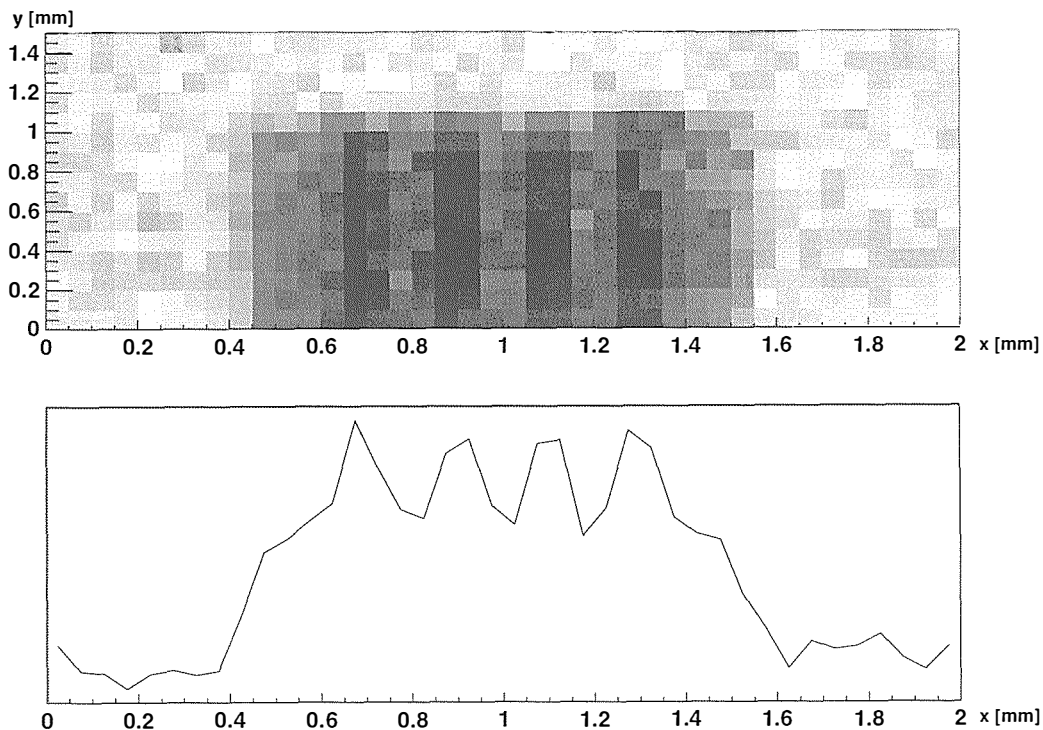


Figure 5. The 5 lp/mm detail from the phantom (Fig. 5a). Due to relatively large, finite size of pixel in x direction ($300\ \mu\text{m}$), the image is distorted. Instead of five lines, separated by $200\ \mu\text{m}$, there are four lines separated by $200\ \mu\text{m}$, superimposed on a plateau (see text below). A x direction cut of Figure 5a at $y = 0.5\ \text{mm}$ is shown in Figure 5b.

expected that the contrast of the images improves, when softer spectrum is used⁹, however at the moment such source is not available to our group.

As our results show, the high efficiency of microstrip detectors can reduce the required dose per investigation. However, when compared to the screen-film, their drawback is a lower spatial resolution. We demonstrated, that 5 lp/mm details (in x direction) can be detected if an appropriate scanning step is chosen. However, due to the large size of pixels, the signal is distorted (Figure 5).

There are still four main improvements which may be implemented. First, a wider and stacked detection system should be assembled in order to reduce imaging time. Stacking 4 to 6 layers of wider detectors would result in a detector covering the area of approx. $1\ \text{mm} \times 5\ \text{cm}$. This would enable imag-

ing of larger objects as well as a reduction of scanning time.

Next, detectors with a lower cutting distance could be used in order to improve efficiency. There are indications that a safe cutting distance could be below $200\ \mu\text{m}$, resulting in detector efficiency above 80% at 20 keV. In comparison, the efficiency of the described detector was about 55%.

The pixel size could be reduced by using thinner silicon substrates (e. g. $200\ \mu\text{m}$) and a finer strip pitch (e. g. $50\ \mu\text{m}$) leading to a better spatial resolution.

Finally, the transfer function of the system must be carefully evaluated and this information used for digital image processing, thus reducing the level of distortion due to the finite pixel size.

With the implementation of all these improvements, the dose required for mam-

mography may be reduced for a factor of about five compared to standard screen film.

References

1. Arfelli F, Barbiellini G, Cantatore G, Castelli E, Cristaudo P, Dalla Palma L et al. Silicon X-ray detector for synchrotron radiation digital radiology. *Nucl Instrum Meth A* 1994; **353**: 366-70.
2. Arfelli F, Barbiellini G, Cantatore G, Castelli E, Cristaudo P, Dalla Palma L et al. Silicon detectors for digital radiography. *Nucl Instrum Meth A* 1995; **367**: 48-53.
3. Beuville E, Cederström B, Danielsson M, Luo L, Nygren D, Oltman E et al. High resolution X-ray imaging using a silicon strip detector. *IEEE T Nucl Sci* 1998; **45**: 3059-63.
4. Mali T, Cindro V, Mikuž M, Richter R. Effect of cutting distance on noise of silicon microstrip detectors. *Proceedings of MIDEM 98 conference, Rogaška Slatina, Slovenia, 1998*: 199-204.
5. Comes G, Loddo F, Hu Y, Kaplon J, Ly F, Turchetta R. CASTOR a VLSI CMOS mixed analog-digital circuit for low noise multichannel counting applications, *Nucl Instrum Meth A* 1996; **377**: 440-5.
6. Colledani C, Comes G, Dulinski W, Hu Y, Loddo F, Turchetta R et al. CASTOR 1.0: A VLSI CMOS mixed analog-digital circuit for pixel imaging applications. *Nucl Instrum Meth A* 1997; **395**: 435-42.
7. Mali T. Postavitev sistema za rentgensko slikanje z mikropasovnimi silicijevimi detektorji. [Diplomsko delo], Ljubljana, Univerza v Ljubljani, 1997
8. Mali T, Cindro V, Mikuž M. X-ray imaging with a silicon microstrip detector. *Proceedings of MIDEM 97 conference, Gozd Martuljek, Slovenia, 1997*: 347-52.
9. Dance DR. Diagnostic radiology with X-rays. In: Webb S, editor. *The physics of medical imaging*. Bristol and Philadelphia: Institute of Physics Publishing; 1988. p. 20-73.
10. Teuber J. *Digital Image Processing*. London: Prentice Hall; 1993.
11. Zavod RS za varstvo pri delu. Sevalna obremenjenost prebivalstva zaradi medicinske uporabe ionizirajočega sevanja v Republiki Sloveniji, poročilo za leto 1996. Ljubljana, 1997.